Laboratory Measurement of Lateral Stress Induced by a Cavity Expansion in a Hollow Cylinder Cell

I. JURAN AND B. MAHMOODZADEGAN

The use of a specially designed hollow cylinder cell in the measurement, under laboratory controlled conditions, of the lateral stress and the excess pore water pressure induced by a cavity expansion in both claycy and granular soils is discussed. The hollow cylinder cell permits the performance of a cavity expansion test in an annular soil specimen under three independent stresses (i.e., axial stress, radial cavity pressure, and lateral confining stress) with measurement of cavity volume change and excess pore water pressures at several locations in the soil specimen. Effective stress analysis of the soil response to the cavity expansion illustrates that the effective lateral stress is independent of the specimen geometry, and intrinsic effective stress-strain relationships can be derived from the experimental expansion curve. However, the specimen geometry does affect the excess pore water pressure generated under undrained conditions, and, therefore, the total stress analysis conventionally used for interpretation of pressuremeter test results is not appropriate for analysis of hollow cylinder cavity expansion test.

Today, pressuremeter and dilatometer tests are being used increasingly to measure the soil response to cavity expansion and to obtain engineering soil properties for design purposes. For fine-grained saturated soils, a total stress interpretation procedure to derive the shear curve (i.e., modulus and undrained cohesion) from the pressuremeter expansion curve was proposed by Baguelin et al. (*1*).

More recently, electric piezo-cells have been incorporated in the pressuremeter probe, as was reported by Baguelin et al. (*2*), Canou and Tumay (*3*), and Juran and Beech (*4*). Measurement of the excess pore water pressure generated by the expanding cylindrical cavity can be used to develop effective stress interpretation procedures capable of providing the in situ effective shear strength characteristics, compressibility, and dilatancy properties of the soil (*4*).

This study has been conducted to investigate the effective lateral stress response to a cavity expansion in both granular and saturated clayey soils. A hollow cylinder cell (HCC) was designed to perform cylindrical cavity expansion tests in annular soil specimens under three independent stresses (i.e., axial stress, radial cavity pressure, and lateral confining stress). The instrumentation of the HCC allows the measurement of the cavity volume change and the excess pore water pressures at three locations within the specimen.

The HCC equipment and its instrumentations have been described by Juran and BenSaid (*5*), who indicated that the procedure proposed by Baguelin et al. (*1*) to derive the intrinsic shear curve of the soil from expansion curves obtained from pressuremeter tests cannot be used for the interpretation of hollow cylinder cavity expansion tests in annual soil specimens of finite dimensions. Juran and BenSaid proposed a total stress analysis procedure that takes into account the effect of sample geometry on the soil response and yields the shear modulus and undrained cohesion of the soil.

This paper focuses on the effective stress analysis of the soil response to cylindrical cavity expansion in the HCC. Interpretation procedures, based on effective stress analysis, are proposed that permit simulation of cavity expansion in both granular and saturated clayey soils. The proposed interpretation procedures are evaluated through the analysis of hollow cylinder cell cavity expansion tests (CETs) in both Fontainbleau sand and silty clay specimens. It is illustrated that the effective lateral stress generated by the cavity expansion is independent of the specimen geometry and that intrinsic effective stress-strain relationships can be derived from the cavity expansion curve. However, the specimen geometry does affect the excess pore water pressure generated under undrained conditions and, therefore, the total stress soil response.

CAVITY EXPANSION TESTS IN A SATURATED CLAYEY SOIL

Laboratory cavity expansion tests, under controlled drainage conditions, yield measurement of the total lateral stress and the excess pore water pressure generated during cavity expansion. Those results can be used for two main purposes: (a) to derive the effective stress-strain relationships of the soil or (b) to evaluate analytical/numerical models developed to predict the lateral stress response of the soil to cavity expansion.

Theoretical Considerations and Interpretation Procedure

The first part of this study focuses on development and evaluation of an effective stress analysis procedure to predict the effective lateral stress generated by the cavity expansion in saturated annular (HCC) specimens of a silty clay. The proposed interpretation procedure is based on the assumptions that follow.

Department of Civil and Environmental Engineering, Polytechnic University, 333 Jay Street, Brooklyn, N.Y. 11201.

Soil Model

A soil model, proposed by Juran and Beech (*4*), is considered, assuming the soil to be an isotropic, elastoplastic, strain-hardening material with a nonassociated flow rule. The strain hardening is assumed to be isotropic, with the hardening parameter being the shear strain defined as

$$\gamma = \frac{1}{\sqrt{2}}[(\varepsilon_1 - \varepsilon_2)^2 + (\varepsilon_2 - \varepsilon_3)^2 + (\varepsilon_3 - \varepsilon_1)^2]^{1/2} \quad (1)$$

where ε_1, ε_2, and ε_3 are the principal strains, with $\varepsilon_1 > \varepsilon_2 > \varepsilon_3$. For a plane strain cylindrical cavity expansion, $\varepsilon_1 = \varepsilon_r$, $\varepsilon_2 = \varepsilon_z$, and $\varepsilon_3 = \varepsilon_\theta$, where ε_r, ε_z, and ε_θ are the radial, vertical, and tangential strains, respectively.

Yield Function

A Mohr-Coulomb-type yield criterion is considered to define the yield surface with an open elastic domain. The assumed yield function can be written as

$$F(\boldsymbol{\sigma},\gamma) = \frac{q - q_0(\gamma)}{p'} - h(\gamma) = 0 \quad (2)$$

where

$\boldsymbol{\sigma}$ = stress tensor,
q = $(\sigma_1' - \sigma_3')/2$ (deviatoric stress),
p' = $(\sigma_1' + \sigma_3')/2$ (average effective stress),
$h(\gamma)$ = strain-hardening function,
$q_0(\gamma)$ = deviatoric stress at $p' = 0$, and
σ_1', σ_3' = major and minor principal stresses, respectively (for cylindrical cavity expansion, $\sigma_1' = \sigma_r'$ and $\sigma_3' = \sigma_\theta'$, where σ_r' and σ_θ' are the effective radial and tangential stresses).

For a contracting (normally consolidated) cohesive soil, the hardening function $h(\gamma)$ is assumed to be of hyperbolic form:

$$h(\gamma) = \frac{\gamma}{a + b\gamma} \quad (2a)$$

with

$$a = \sigma_0'/G \qquad b = 1/\sin\phi_{cv}$$

where

σ_0' = initial consolidation pressure,
G = shear modulus, and
ϕ_{cv} = effective critical state friction angle.

As was indicated by Juran and Beech (*4*), the soil reaches the critical state (i.e., plastic flow at constant volume) at a finite shear strain γ_f, and, therefore, the assumption of a hyperbolic strain-hardening function results in an underestimation of the stress ratio q/p' at large shear strains. Considering this experimental observation, the yield function was modified to take into account the perfectly plastic soil behavior at large strains (i.e., $\gamma > \gamma_f$), assuming that the failure shear strain γ_f is independent of the stress path and a "modified" strain-hardening function is considered.

$$h^*(\gamma) = \frac{\gamma}{a + b^*\gamma} \quad (2b)$$

where

$$a = \sigma_0'/G \qquad b^* = 1/\sin\phi_{cv} - \sigma_0'/G \cdot \gamma_f$$

The hyperbolic and "modified" $h(\gamma)$ functions are illustrated in Figure 1a.

Plastic Flow Function

A stress ratio-dilatancy function of the form proposed by Nova and Wood (*6*) is assumed:

$$\eta = \frac{d\varepsilon_v}{d\gamma^p} = \eta(q/p') \quad (3)$$

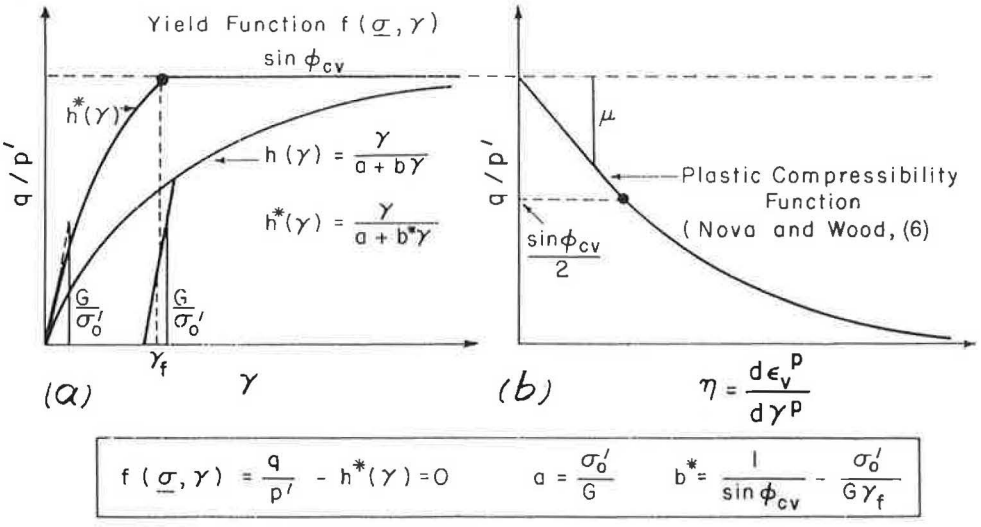

FIGURE 1 Definitions of (a) yield function and (b) stress ratio-dilatancy function.

where $d\varepsilon_v^p$ and $d\gamma^p$ are the plastic volumetric and deviatoric strain increments, respectively. The assumed hyperbolic function $\eta(q/p')$, with an initial linear portion characterized by a contractancy modulus (μ), is schematically illustrated in Figure 1b. As the soil reaches the critical state ($\gamma \geq \gamma_f$), η is equal to zero, indicating no plastic volume change. Having defined $\eta(q/p')$, a nonassociated plastic flow function $Q(q/p')$ can be derived, assuming the coincidence of the axes of principal stresses with those of the corresponding plastic strain increments.

The proposed model defined by Equations 2b and 3 (Figure 1) requires an experimental determination of five soil characteristic parameters: G/σ_0', ν (Poisson's ratio), ϕ_{cv}, γ_f, and μ. If the soil shear strength parameters include a cohesion intercept, then the function $q_0(\gamma)$ must also be determined. Those parameters can be obtained from either triaxial tests (CD test with measurement of the volume change or CU test with measurement of the pore water pressure) or hollow cylinder cell tests with measurement of the pore water pressure generated at the expanding cavity facing.

Effective Stress Analysis Procedure

To simulate numerically an undrained cavity expansion test in a saturated fine-grained soil specimen, the proposed soil model is incorporated in an effective stress analysis procedure. This procedure, an extension of the analytical method proposed by Juran and Beech (*4*) for interpretation of pressuremeter tests in a clayey soil, takes into account the boundary conditions corresponding to the HCC and involves the following steps:

1. A boundary displacement increment Δx_0 is applied at the cavity facing. The induced total strain increments ($d\varepsilon_r$, $d\varepsilon_\theta$) are calculated from the compatibility relationship considering the specific test conditions of vertical plane strain ($d\varepsilon_z = 0$) and undrained expansion ($d\varepsilon_v = 0$). The shear strain increment $d\gamma$ at a radial coordinate r is given by

$$d\gamma(r) = \sqrt{3}\, d\varepsilon_\theta = \sqrt{3}\,\frac{\Delta x_0 r_0}{r^2} \tag{4a}$$

at the cavity facing ($r = r_0$)

$$d\gamma(r_0) = \sqrt{3}\,\frac{\Delta x_0}{r_0} \tag{4b}$$

2. The test conditions (i.e., $d\varepsilon_z = 0$, $d\varepsilon_v = 0$) yield the following expression for the $\left(\frac{q}{p'}\right)$ function:

$$\eta = \frac{d\varepsilon_v^p}{d\gamma^p} = \frac{d\varepsilon_v - d\varepsilon_v^e}{d\gamma \quad d\gamma^e} = \frac{\left(\frac{1-2\nu'}{G}\right)\cdot\left(\frac{dp'}{d\gamma}\right)}{1-\left(\frac{1}{2G}\right)\cdot\left(\frac{d\tau_{oct}}{d\gamma}\right)} \tag{5a}$$

or

$$d\gamma = -\left(\frac{1-2\nu'}{G\eta}\right) dp' + \left(\frac{1}{2G}\right) d\tau_{oct} \tag{5b}$$

where

$d\varepsilon_v$, $d\varepsilon_v^e$ = total and elastic volumetric strain increments, respectively,
$d\gamma$, $d\gamma^e$ = total and elastic shear strain increments, respectively, and
$\tau_{oct} = 1/\sqrt{2}\,[(\sigma_r - \sigma_\theta)^2 + (\sigma_\theta + \sigma_z)^2 + (\sigma_z - \sigma_r)^2]^{1/2}$ (octahedral shear stress).

The vertical plane strain condition implies $\sigma_\theta = \nu'(\sigma_r + \sigma_z)$, and, therefore,

$$\tau_{oct} = p'[3h^*(\gamma) + (1 - 2\nu')^2]^{1/2} \tag{6}$$

3. The constitutive equations (i.e., Equations 2b and 3) derived from triaxial test results, coupled with Equations 5b and 6 provide a solution for the effective stress increments at the cavity facing, $d\sigma_r'(r_0)$ and $\sigma_\theta'(r_0)$, as a function of the shear strain.

As will be indicated, the solution for the effective stresses at the cavity facing is independent of the sample geometry and the boundary conditions applied at the external facing of the specimen. Therefore, the HCC can be adequately used to evaluate numerical models and analytical procedures developed to predict the effective stress soil response. However, the sample geometry and the boundary lateral stress do affect the excess pore water pressures generated by the cavity expansion and, thus, the total stress response.

4. The shear strain variation $\gamma(r)$ throughout the sample can be determined from Equation 4a. The solution derived for the effective stresses at the cavity facing can then be used to establish the variation of effective stresses [$q = q(r)$, $p' = p'(r)$] as a function of the spatial coordinate r.

5. The total stress increment $d\sigma_r$ can be calculated from the radial equilibrium condition

$$\frac{d\sigma_r}{d\rho} + \frac{2q}{\rho} = 0 \tag{7}$$

(where ρ is the actual radius) considering the boundary conditions $d\sigma_r(R) = 0$, where R is the external radius of the specimen.

The excess pore water pressure is given by

$$u(\rho) = \sigma_r(\rho) - \sigma_r'(\rho) \tag{8}$$

recalling that

$$\sigma_r'(\rho) = q(\rho) + p'(\rho) \tag{9}$$

Experimental Study

The soil used in this part of the study was a low plasticity silty clay with liquid and plastic limits of 35 percent and 21 percent, respectively. The grain size distribution of this soil contains 95 percent < 80 μm, 50 percent < 2 μm, and 26 percent < 0.2 μm.

Soil Properties

Triaxial undrained (CU) and drained (CD) tests were performed to obtain the material properties for the proposed soil model (i.e., Equations 2b and 3). Figure 2 presents the typical results of CU tests on two lightly overconsolidated specimens of the soil used in this study. In the q-p' plane, the effective stress paths followed by the soil in different tests are geometrically similar, and the "iso-γ" curves can be approximated by straight lines (Equation 2). For normally consolidated specimens, $q_0(\gamma) = 0$. Figure 2 also illustrates that the stress paths actually reach the failure envelope at a finite shear strain γ_f of about 8 percent, contrary to the assumption of the hyperbolic model that implies $\gamma_f = \infty$.

Figure 3 illustrates the strain-hardening function $h^*(\gamma)$ and the stress ratio-dilatancy relationship $\eta(q/p')$ derived from the results of the triaxial CU and CD tests. CU and CD tests yield nearly an identical $h^*(\gamma)$ function. However, a significant difference exists in the $\eta(q/p')$ functions obtained from the results of those two tests. The contractancy modulus (μ) values obtained from the CU test results were found to be significantly greater (i.e., 2.5 to 2.9) than those obtained from the CD tests (i.e., 1.0 to 1.2). This substantial difference in the experimentally determined μ values indicates that in a normally consolidated clay the $\eta(q/p')$ function appears to be stress-path dependent.

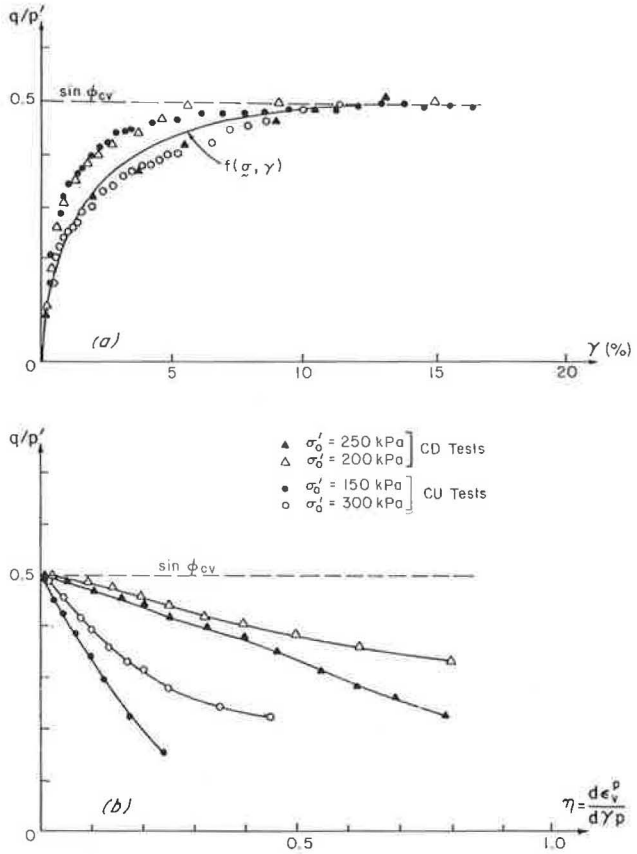

FIGURE 3 (a) Strain-hardening and (b) stress ratio-dilatancy functions derived from triaxial CU tests results.

Cavity Expansion Tests

To investigate the validity of the proposed effective stress analysis procedure, cavity expansion tests (CETs) were performed in a specially designed HCC. Figure 4 presents a schematic view of the HCC and its instrumentation (*5*).

In this cell, an annular soil specimen (internal and external radii of 1 and 5 cm, respectively) is subjected to three independent stresses: the axial stress, σ_z; the radial cavity pressure, σ_c; and the lateral confining stress, σ_R. The cell is equipped with three pore water pressure transducers located at the bottom of the cell at distances of 16, 30, and 44 mm from the cavity center. The volume changes of both the soil and the internal cavity are recorded during the expansion test. A cavity expansion curve relating the applied cavity pressure σ_c to the cavity volume change Δv_c is obtained, which is similar to typical results of in situ self-boring pressuremeter tests (*1*).

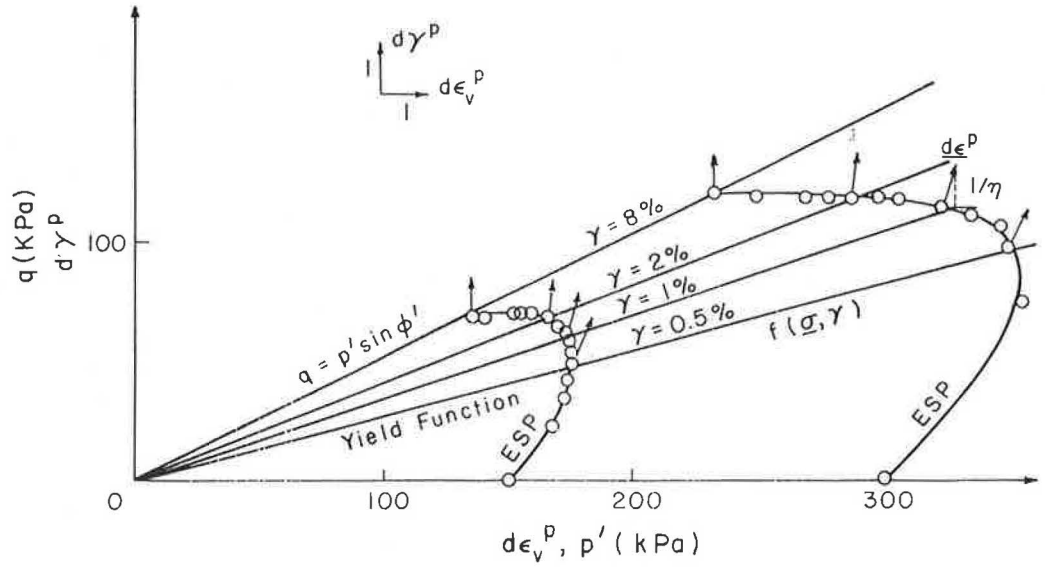

FIGURE 2 Effective stress paths obtained from triaxial CU tests on specimens of a silty clay.

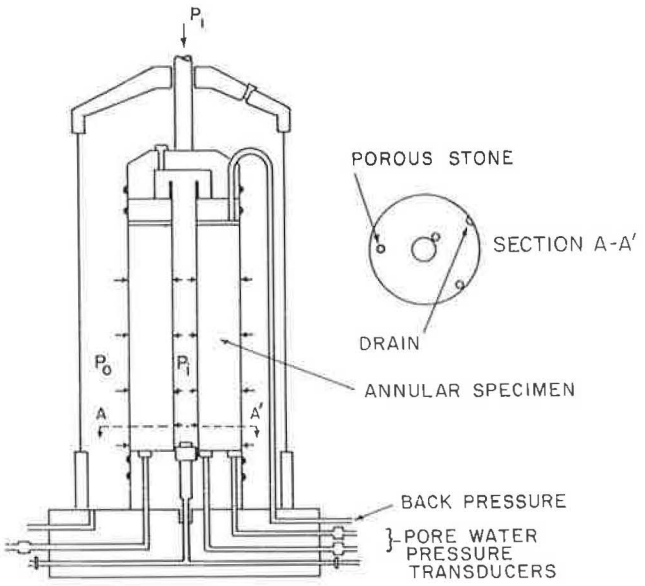

FIGURE 4 Cross-sectional scheme of the hollow cylinder cell [after Juran and BenSaid (5)].

Figure 5 presents typical results of an undrained CET with initial consolidation pressure of $P_0' = 250$ kPa. In addition to the expansion curve and the measured excess pore water pressures, the measured vertical strain is presented in this figure. As observed, the maximum vertical strain measured during this test was less than 1 percent, which is an indication of the validity of the plane strain assumption for the test conditions of the HCC.

Figures 6 and 7 present the cavity expansion curves and the excess pore pressures at the cavity facing measured during two additional CET tests with initial consolidation pressures of 150 and 200 kPa, respectively.

Analysis of the CET Results

The proposed effective stress analysis procedure permits simulation of the effective radial stress response to a cavity expansion in the annular HCC specimen and requires an appropriate determination of the soil constitutive equations (2b and 3) from the results of triaxial CU and CD tests. However, analysis of the triaxial test results (Figure 3) illustrate that for the normally consolidated clay specimens, while a rather unique $h^*(\gamma)$ function can be obtained, the derived stress ratio-dilatancy relationship $\eta(q/p')$ appears to be stress path dependent. Therefore, in evaluating the proposed procedure, rather than arbitrarily selecting a $\eta(q/p')$ function to predict the effective lateral and tangential stress (i.e., σ_r', σ_θ') response, an attempt is made to compare the $\eta(q/p')$ function obtained directly from the CET results with those derived from the triaxial CU and CD tests.

To determine the stress ratio-dilatancy function directly from the cavity expansion test results, Equations 5a and 6 were used simultaneously, along with the $h^*(\gamma)$ function determined from the triaxial CU and CD test results. Figure 8a illustrates that the stress ratio-dilatancy function $\eta(q/p')$ determined from the CET results ($1.5 < \mu < 2.0$) lies within

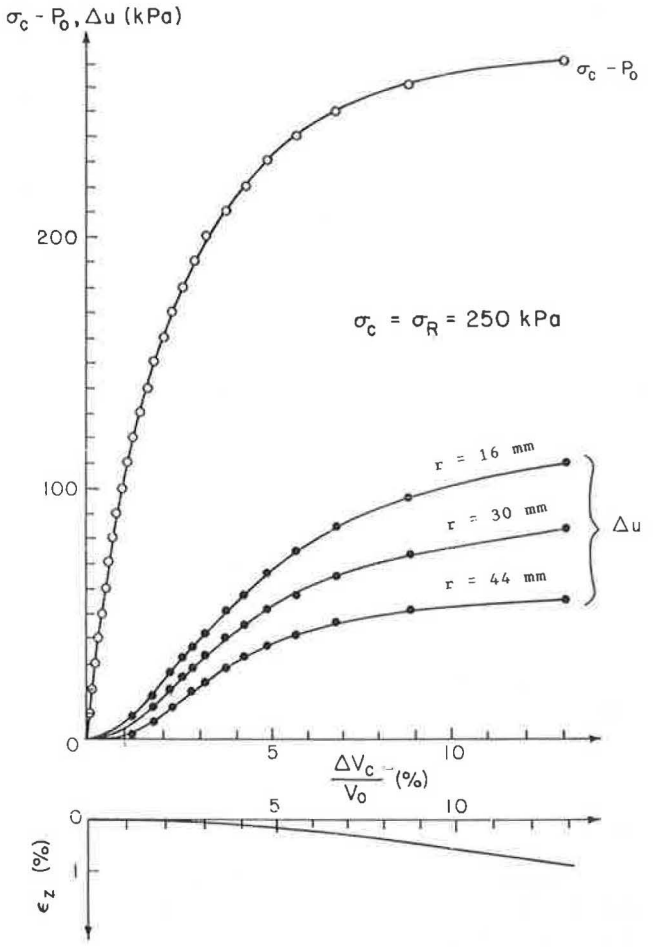

FIGURE 5 Typical results of an undrained cavity expansion test.

a range bounded by those obtained from triaxial CU ($2.5 < \mu < 2.9$) and CD ($1.0 < \mu < 1.2$) tests. Those results are consistent with the effective stress paths, obtained for those three types of tests, as is indicated in Figure 8a for $P_0' = 250$ kPa.

The proposed effective stress analysis was used, considering the obtained $\eta(q/p')$ function and taking μ values of 1 and 2, to simulate the cavity expansion tests conducted with $p_0' = 150$ and 200 kPa. Figures 9 and 10 present the comparison between the predicted and measured total lateral stress response and the generated excess pore water pressures for the two tests. Those comparisons illustrate that with the derived μ value ($1.5 < \mu < 2.0$), the proposed model will predict fairly well the range of the excess pore water pressures generated by the cavity expansion. However, the lateral stress soil response is underestimated. For a value of contractancy modulus (μ) of 2, the difference between the predicted and experimental lateral stress response curves (Figure 9a) attains a maximum of about 15 percent. This difference is partially due to sample preparation effects that result in local heterogeneities within the specimen. Such heterogeneities were evidenced by irregularities in the cavity shape at the completion of the test. End effects were minimized, using a double membrane system lubricated with grease. However, the difference between the predicted and experimental results also can be attributed to

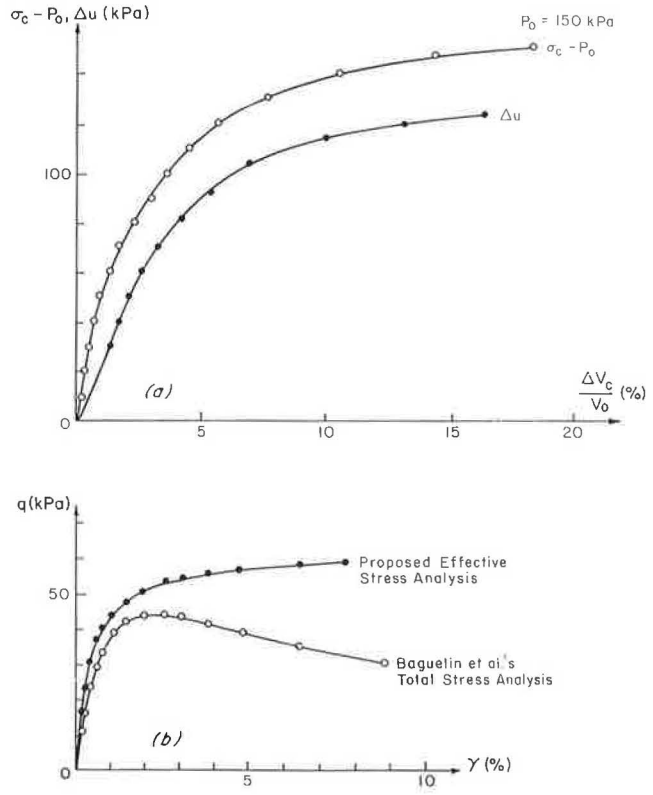

FIGURE 6 (a) Cavity expansion test results under $P_0' = 150$ kPa and (b) comparison of the derived shear curves by using effective and total stress analyses.

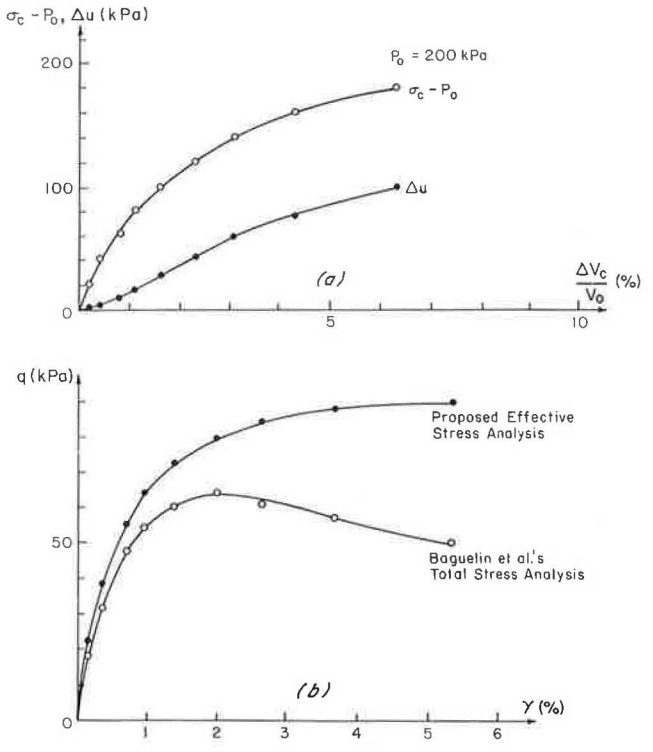

FIGURE 7 (a) Cavity expansion test results under $P_0' = 200$ kPa and (b) comparison of the derived shear curves by using effective and total stress analyses.

the limitations of the proposed soil model and particularly to the high sensitivity of the predicted results to small variations in μ values.

Evaluation of the Specimen Geometry Effect on the Derived Shear Curve

Interpretation of cavity expansion curves produced by pressuremeter in saturated clayey soils is conventionally based on the total stress analysis procedure proposed by Baguelin et al. (*1*). This analysis procedure is derived by using the radial equilibrium and compatibility equations, assuming that a unique shear curve $q = g(\varepsilon_\theta)$ can be obtained for the saturated incompressible semi-infinite soil medium, which would be independent of the spatial coordinate r. This shear curve can be expressed as

$$q = \frac{d(\sigma_c - p_0)}{dg_0} g_0(1 + 2g_0) \tag{10}$$

where

$$g_0 \cong \varepsilon_\theta = \frac{\sqrt{3}}{3}\gamma \tag{11}$$

Because the HCC specimen does not represent a semi-infinite medium, the shear curve derived from this total stress analysis is not unique. In particular, at the external facing of the specimen ($r = R$), the boundary conditions imply $d\sigma_R = 0$ while $d\varepsilon_\theta = dx_R/R$ (dx_R and $d\sigma_R$ are the radial displacement and the lateral stress increments at $r = R$, respectively). Therefore, this total stress analysis does not permit an appropriate consideration of the effect of specimen geometry and the boundary conditions on the soil response to cavity expansion.

To evaluate the effect of specimen geometry, the shear curves derived from the HCC test results, using Baguelin's procedure, are compared with reference shear curves. Those reference curves were established by coupling the soil strain-hardening function, obtained from triaxial tests, with the effective lateral stress measured at the cavity facing. The equation used to determine the reference shear curves is independent of the boundary conditions and can be written as

$$q = p' \cdot h^*(\gamma) = \frac{h^*(\gamma)}{1 + h^*(\gamma)}[\sigma_c - \Delta u] \tag{12}$$

Figures 6b and 7b illustrate the comparisons between the shear curves obtained by using Equations (10) and (12) for the cavity expansion tests conducted under $p_0' = 150$ and 200 kPa. Those comparisons illustrate the substantial effect of the analysis procedure on the derived shear curve, indicating that the specimen geometry significantly affects the total stress soil response to cavity expansion.

To investigate the specimen geometry effect further, the test conducted under $p_0' = 150$ kPa was numerically simulated for increasing values of the external to internal specimen radius ratios (R/r_0). The results of those simulations (Figure 11) indicate that a unique lateral effective stress curve is obtained

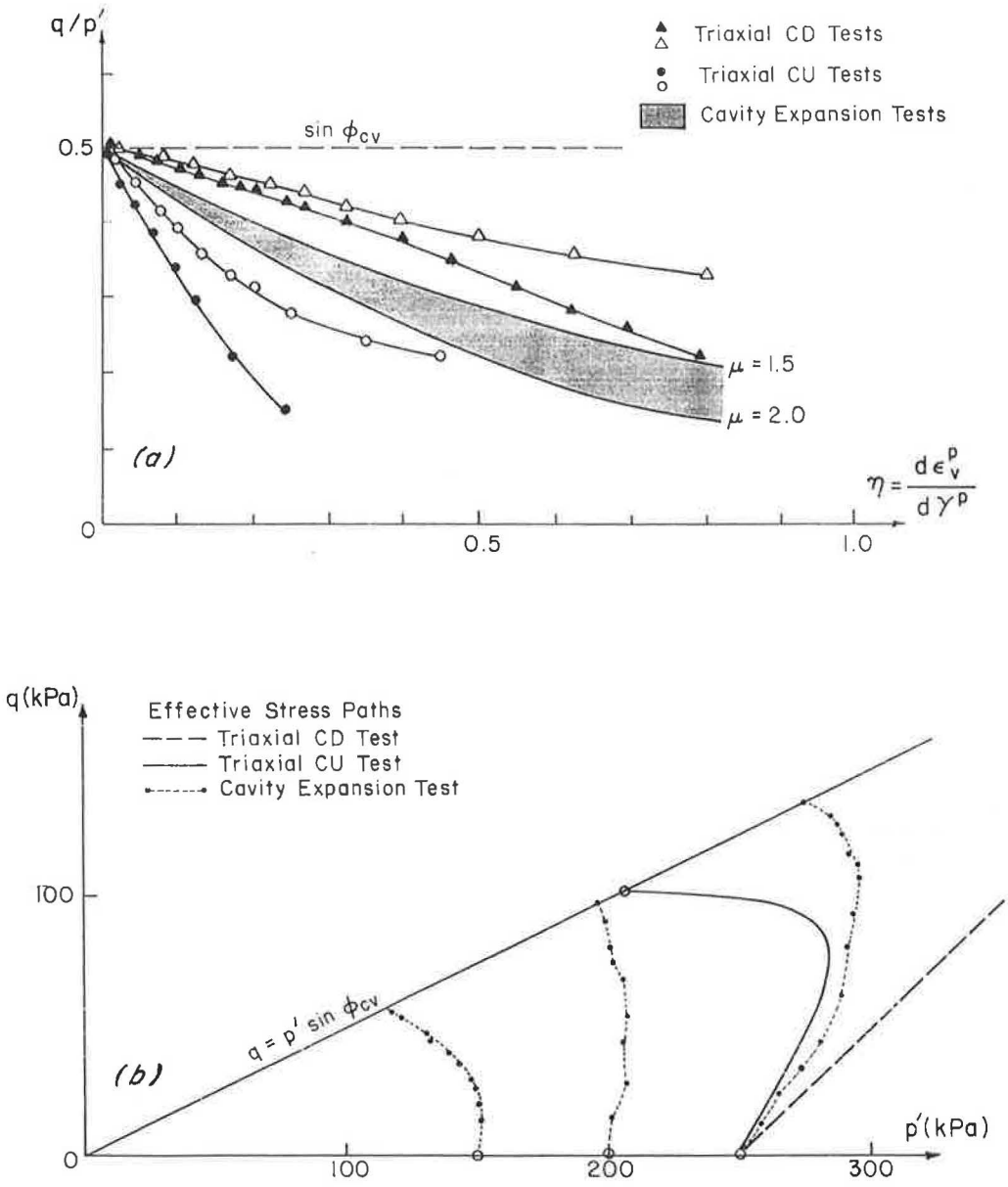

FIGURE 8 Comparisons of (a) the derived stress ratio-dilatancy functions and (b) the effective stress paths from triaxial CU, CD, and cavity expansion tests.

and the total stress and excess pore water pressure depend on the specimen geometry. An increase in the R/r_0 ratio of 5 to 50 results in an increase of only 10 percent in the total lateral stress and an equal decrease of the excess pore water pressure.

Figure 12 presents the shear curves derived from the theoretical expansion curves in Figure 11, using Baguelin et al.'s total stress analysis. Those results indicate, that as the R/r_0 increases the shear curves approach the reference shear curve.

The results presented in Figures 11 and 12 indicate that the specimen geometry has no effect on the effective lateral stress response of soils to cavity expansion but can significantly affect the total lateral stress response and the generated excess pore water pressure.

CAVITY EXPANSION TESTS IN SANDS

Theoretical Considerations and Interpretation Procedure

The soil model described earlier was extended by Juran and Mahmoodzadegan (*7*) for analysis of cavity expansion tests in sands. This soil model, which takes into account the dilating and contracting sand behavior or both, was incorporated in an analysis procedure for interpretation of pressuremeter tests in sands. This analysis procedure, derived from the compatibility and the radial equilibrium conditions for cylindrical cavity expansion, yields an expression for the shear curve,

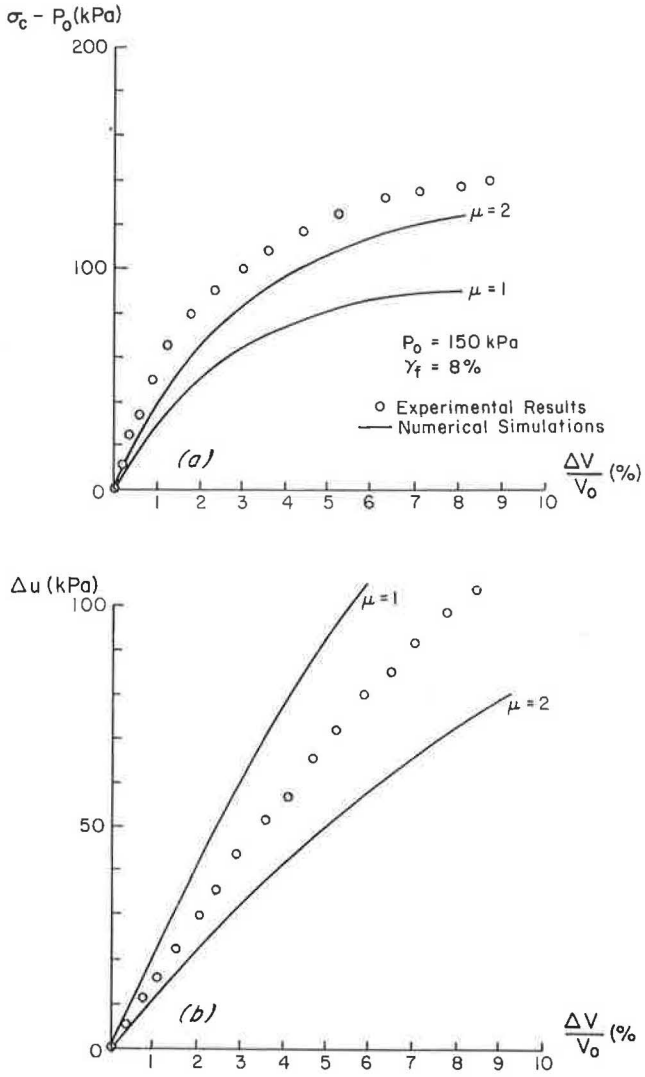

FIGURE 9 Comparisons of (a) the experimental and predicted expansion curves and (b) experimental and predicted excess pore water pressure curves under $P_0' = 150$ kPa.

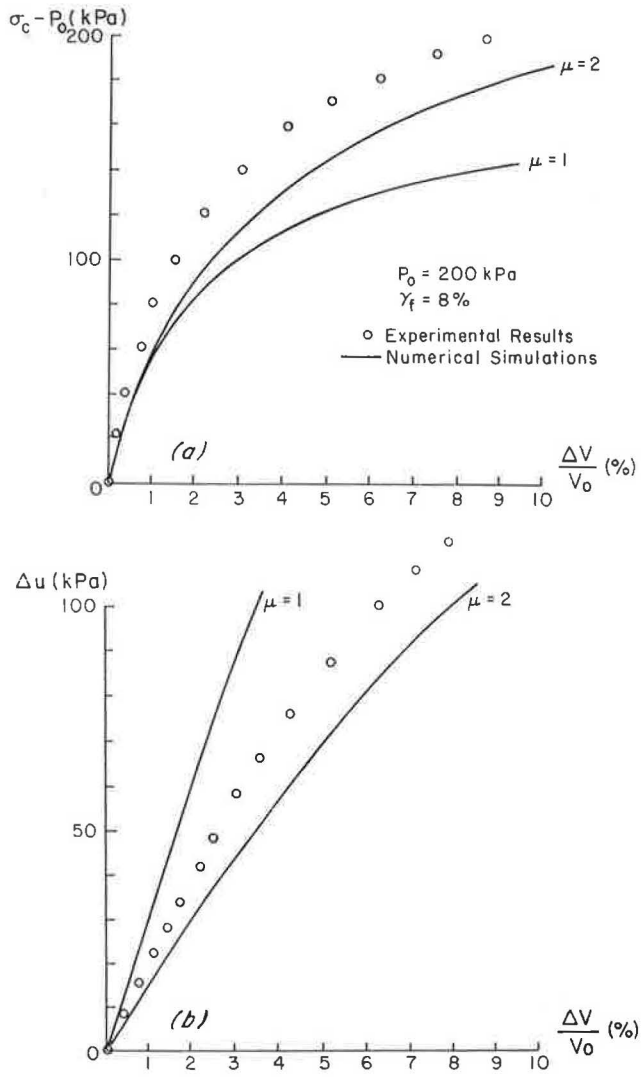

FIGURE 10 Comparisons of (a) the experimental and predicted expansion curves and (b) experimental and predicted excess pore water pressure curves under $P_0' = 200$ kPa.

which can be incrementally derived as

$$q = \frac{\partial(\sigma_c - P_0)}{\partial \varepsilon_\theta} \cdot \frac{\varepsilon_\theta}{1 - \sin \xi} \cdot \frac{1 + \varepsilon_\theta}{1 - \varepsilon_\theta} \tag{13}$$

where

$$\sin \xi = \sin \psi - \gamma \cdot \frac{\partial(\sin \xi)}{\partial \gamma} \tag{14a}$$

and ψ is the dilation angle of the sand that can be obtained from the following relationship:

$$\sin \psi = 1 + 2 \frac{d\varepsilon_\theta}{d\gamma} \tag{14b}$$

Equation 13 is obtained independently of any assumption regarding the constitutive equation of the soil.

At the cavity facing, the radial stress σ_r is equal to the applied cavity pressure σ_c. The average effective stress at this location is, therefore, given by

$$p' = (p_0 + \Delta\sigma_c) - q - \Delta u \tag{15}$$

where Δu is the excess pore water pressure generated at the cavity facing, $\Delta\sigma_c$ is the applied cavity pressure increment, and p_0 is the initial cavity pressure.

Coupling Equations 12, 13, and 15 with the constitutive equations of the soil yields the following incremental relationship for the effective lateral stress in the soil:

$$\frac{\Delta(\sigma_c - p_0)}{\Delta \varepsilon_\theta} = \frac{1 - \sin \xi}{1 + h^*(\gamma)} \cdot \frac{h^*(\gamma)}{\varepsilon_\theta} \cdot \frac{1 - \varepsilon_\theta}{1 + \varepsilon_\theta} [\sigma_c - \Delta u] \tag{16}$$

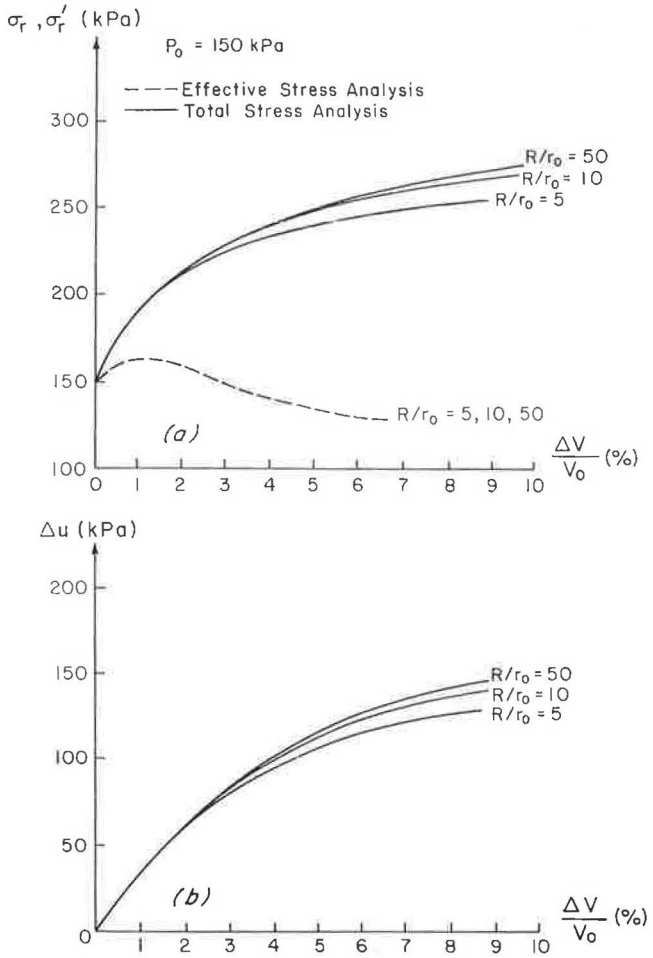

FIGURE 11 Effect of specimen geometry on (a) the lateral stress and (b) the excess pore water pressures.

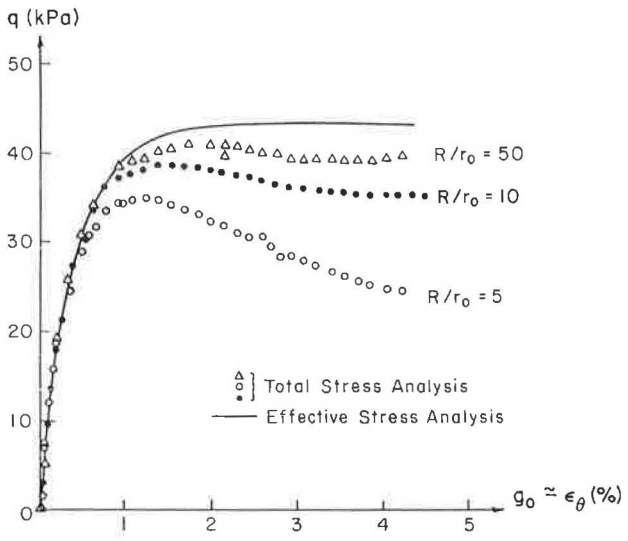

FIGURE 12 Comparison of the shear curves determined by using total and effective stress analysis procedures.

Equations 13 and 15 allow determination of the soil properties (i.e., shear strength characteristics, dilation properties, and shear modulus) through an analysis of CET results. Equation 16 permits simulation of the CET in an annular specimen of a soil with given constitutive equations (i.e., strain-hardening function and stress ratio-dilatancy relationship).

Analysis of CET Results

To evaluate the proposed interpretation procedure, laboratory cavity expansion tests were performed on Fontainbleau sand specimens in an HCC (*8*).

The soil used in this study was a fine Fontainbleau sand (average grain diameter of 0.10 mm) of which the mechanical properties were obtained from the analysis of consolidated drained triaxial test results reported by Habib and Luong (*9*). Figures 13a and 13c present the stress ratio-shear strain curves [$q/p' = h(\gamma)$] and the volumetric strain-deviatoric strain curves [$\varepsilon_v = f(\gamma)$] obtained under confining pressures of σ_0' = 100, 300, and 600 kPa. The figures illustrate the effect of confining pressure on the peak shear strength characteristics and volume change properties of this sand. Figure 13b indicates that in spite of significant differences in volume changes measured in those three tests the confining pressure has a rather minor effect on the stress ratio-dilatancy relationship $\eta(q/p')$, which can be approximately represented by a bilinear curve with a contractancy modulus μ_1 and a dilatancy modulus μ_2. The experimental curves are compared with numerical simulations by using the proposed soil model with the following mechanical properties:

1. For σ_0' = 300 kPa: G/σ_0' = 60, ϕ = 39.5 degrees, ϕ_{cv} = 32.5 degrees, μ_1 = 2, μ_2 = 0.85 and
2. For σ_0' = 600 kPa: G/σ_0' = 60, ϕ = 37 degrees, ϕ_{cv} = 32.5 degrees, μ_1 = 1.7, μ_2 = 1.0.

As is indicated in Figure 13, the model predictions agree fairly well with the experimental results. For the sake of analysis, the following average soil properties are considered: G/σ_0' = 60, ϕ = 38.5 degrees, ϕ_{cv} = 32.5 degrees μ_1 = 1.8, and μ_2 = 0.9.

The hollow cylinder cells with internal to external radius ratios, τ_0/R, of 1.5 and 1.10 were used in those tests to evaluate the effect of the boundary conditions on the effective stress response of the sand.

Figure 14 presents typical results of an undrained expansion test, including an expansion curve and measured excess pore water pressures. The measured excess pore pressures illustrate that in this highly permeable sand the gradient of the generated excess pore pressures dissipate instantaneously and the pore pressures become uniform throughout the specimen. Therefore, the measured excess pore water pressures are indicative only of the global tendency of the sand specimen to dilate during expansion, while locally the sand can be contracting or dilating depending on the actual shear strain level at the specific point (r) under consideration. The vertical displacement measured during the tests were found to be very small, illustrating a plane strain expansion.

Figure 15 illustrates the comparison of the experimental and predicted cavity expansion curves obtained by using the

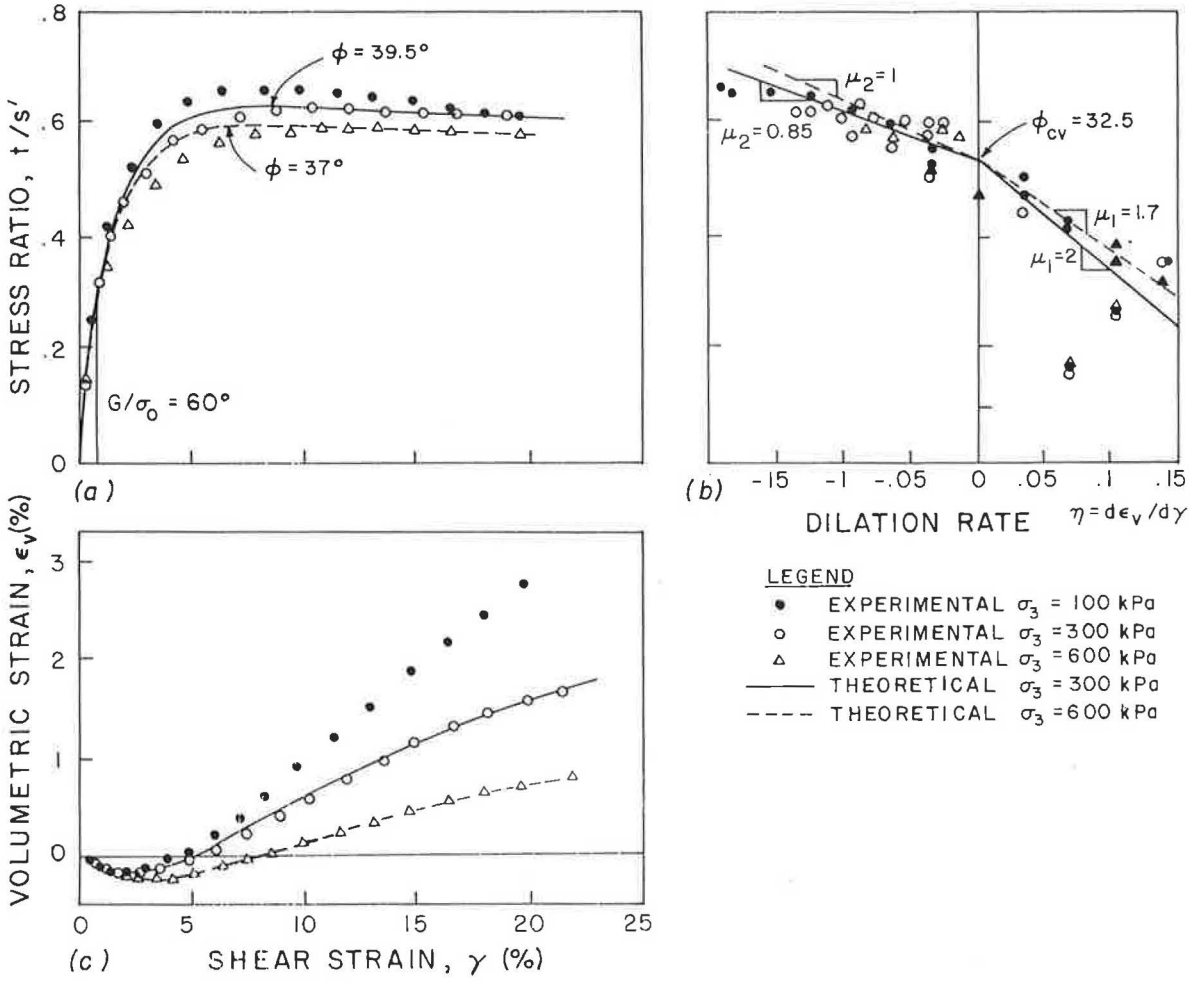

FIGURE 13 Prediction of the response of the Fontainbleau sand during triaxial compression tests.

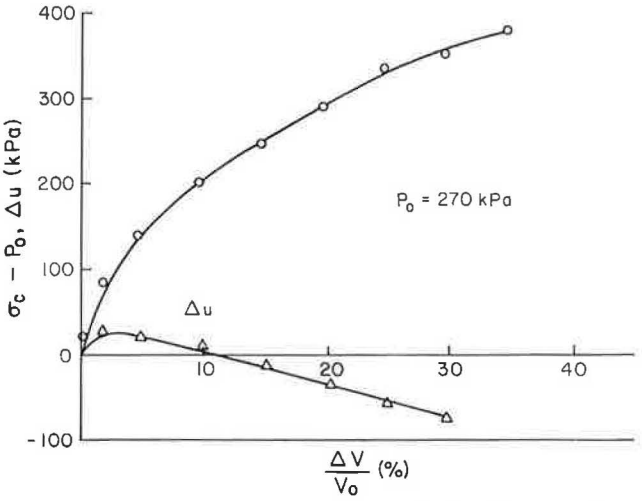

FIGURE 14 Typical results of an undrained cavity expansion test on a Fontainbleau sand specimen.

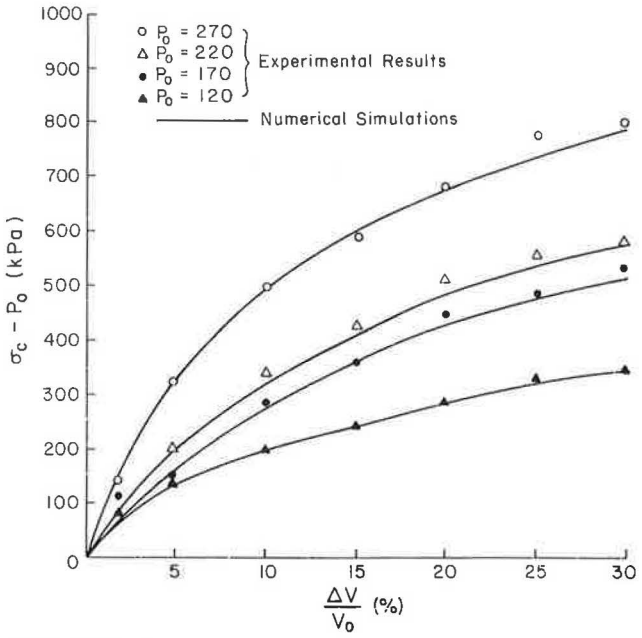

FIGURE 15 Comparison of the experimental expansion curves with numerical predictions by using the proposed procedures.

proposed interpretation procedure with the soil properties indicated before that in spite of the substantial differences in the effective stress paths followed during the triaxial CD and the cavity expansion tests (7) the proposed interpretation procedure predicts fairly well the experimental results. Those results indicate that for dense dilating sands the assumed constitutive equations (i.e., strain-hardening function and stress ratio-dilatancy relation) are rather stress-path independent. This analysis also illustrates that the specimen geometry has practically no effect on the stress response of the sand. Therefore, in spite of basic differences in boundary conditions between the laboratory specimen and the in situ semi-infinite soil medium, the proposed procedure is anticipated to be relevant for interpretation of pressuremeter tests in sandy soils.

SUMMARY AND CONCLUSIONS

The HCC equipment developed for the purpose of this study permits laboratory simulation of the soil response to cavity expansion and provides an appropriate means for evaluating analytical/numerical models that have been developed to predict the total and effective lateral stress soil response of both saturated clayey and sandy soils.

An interpretation procedure for cavity expansion test in the HCC has been developed and allows evaluation of the effect of the boundary conditions and specimen geometry on the effective and total lateral stresses and on the excess pore water pressures generated in the soil.

A laboratory study has been conducted to evaluate the proposed interpretation procedure. The analysis of the test results has demonstrated that the lateral effective stress response in saturated clayey soils (or the total/effective lateral stress response in sandy soils) is independent of specimen geometry and boundary conditions. Therefore, it is anticipated that (a) the proposed effective stress analysis procedure would be relevant for interpretation of (in situ) pressuremeter tests results and that (b) the effective stress-shear strain relationships derived from the laboratory cavity expansion tests could be extrapolated to field conditions.

Analysis of the test results has also shown that in saturated clayey soils specimen geometry and boundary conditions may significantly affect the total stress and excess pore water pressure generated during cavity expansion. Therefore, the total stress analysis conventionally used in interpretation of pressuremeter tests is not appropriate for the analysis of a laboratory cavity expansion test in the HCC.

The proposed interpretation procedure incorporates a relatively simple elastoplastic soil model with a nonassociated flow rule. Analysis of triaxial CU, CD, and undrained cavity expansion tests in the HCC has demonstrated that in normally consolidated clayey soils the assumed stress ratio-dilatancy function appears to be stress path dependent and the predicted cavity expansion curves are highly sensitive to the value of the contractancy modulus. In dilating sands, however, the assumed $\eta(q, p')$ function appears to be stress-path independent, and the proposed model predicts the experimental results fairly well.

Finally, in light of differences between the laboratory reconstituted specimens and the in situ soil (e.g., depositional history, fabric, in situ stress state), field testing is required for further evaluation of the proposed procedure to predict the in situ lateral stress soil response.

REFERENCES

1. F. Baguelin, J. F. Jezequel, and D. H. Shields. *The Pressuremeter and Foundation Engineering*. Trans Tech Publications SA, Clausthal, Germany, 1978.
2. F. Baguelin, J. F. Jezequel, and Le Mehaute. Etude des Pressions Interstitielles Developées lors de l'Essai Pressiometrique. *Proc., 8th ICSMFE*, Moscow, 1973.
3. J. Canou and M. T. Tumay. Field Evaluation of French Self-boring Pressuremeter PAF-76 in a Soft Deltaic Louisiana Clay. *Proc., 2nd ISPMT*, Texas A&M University, 1986, pp. 97–118.
4. I. Juran and J. F. Beech. Effective Stress Analysis of Soil Response in a Pressuremeter Test. *Proc., Pressuremeter and Its Marine Applications, Second International Symposium*, ASTM STP 950, 1986, pp. 150–168.
5. I. Juran and M. A. BenSaid. Cavity Expansion Tests in a Hollow Cylinder Cell. *Geotechnical Testing Journal*, Vol. 10, No. 4, 1987, pp. 203–212.
6. R. Nova and D. M. Wood. A Constitutive Model for Sand in Triaxial Compression. *Int. J. Num. Anal. Meth. Geomech.*, Vol. 3, 1979.
7. I. Juran and B. Mahmoodzadegan. Interpretation Procedure for Pressuremeter Tests in Sand. *Journal of the Geotechnical Engineering Division*, ASCE, Vol. 115, No. 11, 1989, pp. 1617–1632.
8. M. A. BenSaid. Mesures In Situ des Pressions Interstitielles: Application a' la Reconnaissance des Sols. Ph.D. dissertation. CERMES, ENPC, Paris, 1986.
9. P. Habib and M. P. Luong. Sols Pulverulents sous Chargements Cycliques. Presented at Seminaire Materiaux et Structures Sous Chargement Cycliques, Ecole Polytechnique, France, 1979.

Publication of this paper sponsored by Committee on Soil and Rock Properties.